THE JOURNAL OF PHYSICAL CHEMISTRY B

Article

pubs.acs.org/JPCB

Excess Dynamic Stokes Shift of Molecular Probes in Solution

Mohsen Sajadi*,† and Nikolaus P. Ernsting*

Department of Chemistry, Humboldt-Universität zu Berlin, Brook-Taylor-Strasse 2, D-12489 Berlin, Germany

Supporting Information

ABSTRACT: The solvation dynamics of molecular probes is studied by broad-band fluorescence upconversion. The time-dependent position of the $S_1 \rightarrow S_0$ emission band or of a vibronic line shape is measured with ~80 fs, 10 cm^{-1} resolution. Polar solutes in acetonitrile and acetone, when excited into S_1 with excess vibrational energy, show a dynamic Stokes shift which extends to the red beyond the quasistationary state. Equilibrium is then reached by a slower blue shift on a 10 ps time scale. In methanol, excess vibrational energy as large as ~14 000 cm^{-1} shows no such effect. Nonpolar solutes exhibit an excess red shift of the emission band in both polar and nonpolar solvents even upon excitation near the vibronic origin. The observed dynamics are discussed in terms of transient heating of the excited chromophore, conformational change, and changes of the molecular cavity size. For solvation studies the optical excitation should be chosen close to the band origin.

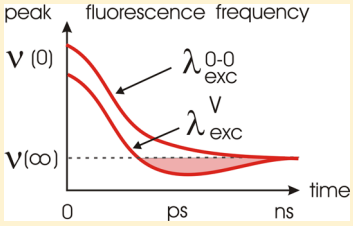

INTRODUCTION

The solvation dynamics of polyatomic molecular probes in conventional solvents has been studied extensively over the past few decades.[1−5] Early experiments succeeded in resolving the diffusive portion of the dynamic fluorescence Stokes shift.[6,7] With advances in time-resolved techniques and improved measurement accuracy, more complex behavior of the shift was revealed.[1,8] Progress along this line eventually yielded the complete ultrafast response of small solvents such as acetonitrile[1] and water[9] to a sudden change of the probe charge distribution. The initial response can be described by a Gaussian time function and is attributed to "free-steaming" inertial motion of the solvent molecules.[10,11] On an intermediate time scale, coherent rotational motion of several solvent molecules may occur. Experimentally, such motion was seen for the first time in a broad-band emission study of 2-amino-7-nitrofluorene in acetonitrile,[12] an observation which had been predicted by molecular dynamics simulations earlier.[10,13]

The dynamic Stokes shift is defined with the help of $\nu_{00}(t)$, the frequency of the electronic origin transition for the evolving emission band, but molecular probes in solution show little or no vibrational structure so that the origin cannot be identified directly. As a substitute one therefore takes the peak $\nu_p(t)$ of the emission envelope or its first moment $\overline{\nu}(t)$.[1] If such a time function is to be determined with some confidence, clearly at every instant the shape of the fluorescence band must be monitored[14−16] with corresponding accuracy.

Over the past few years, we have developed a fluorescence upconversion setup with which one can watch entire transient fluorescence bands with 80 fs temporal resolution.[17] When such a band is fitted by a log-normal function,[1] for example, the residual noise (rmsd) is less than 2% of the peak signal. For a typical fluorescence spectrum this translates into a precision for determining the peak frequency ν_p of ±10 cm^{-1} (68% confidence interval). Since it is the change of peak frequency which enters the dynamic Stokes shift, the latter is determined with corresponding precision. In this way the solvation dynamics can be characterized in unprecedented detail.[18,19]

Here we examine the effect of excess vibronic energy when polar probes are photoexcited in aprotic and protic polar solvents. As a new phenomenon an "excess" red shift is reported for the early part of the response, followed by a "reverse" blue shift to reach the stationary state. We extend this study to nonpolar solutes where the experimental data are available only for relatively viscous solvents and spectral resolution is limited due to small Stokes shifts.[20−23] The observed dynamics are discussed in terms of nonspecific interaction between the solute and solvent, changes of the molecular cavity, and cooling following optical excitation.

EXPERIMENTAL SECTION

Materials. The chemical structures of the solutes in this study are shown in Scheme 1. Coumarins C343, C153, and C334 were obtained from Radiant Dyes, 3-aminophthalimide (3AP), 2,5-bis(5-*tert*-butyl-2-benzoxazolyl)thiophene (BBOT), and perylene were obtained from Aldrich, and 4-(dicyanomethylene)-2-methyl-6-(*p*-(dimethylamino)styryl)-4*H*-pyran (DCM) was obtained from Lambda Physik. The dyes were used as received. Stationary absorption and emission spectra, as functions of the wavelength λ, were recorded with a Cary 300 spectrometer and a Spex 212 fluorometer, both with 1 nm resolution.

Broad-Band Fluorescence Upconversion was performed with the setup and procedures reported elsewhere.[17] With a BBO crystal and angular predispersion of fluorescence by a calcite wedge, the sensitivity was increased and phase matching was widened. Dyes were dissolved so that the optical density at

Received: January 15, 2013
Revised: May 29, 2013
Published: May 30, 2013

 © 2013 American Chemical Society

Scheme 1. Chemical Structures of the Molecular Probes Used in This Study

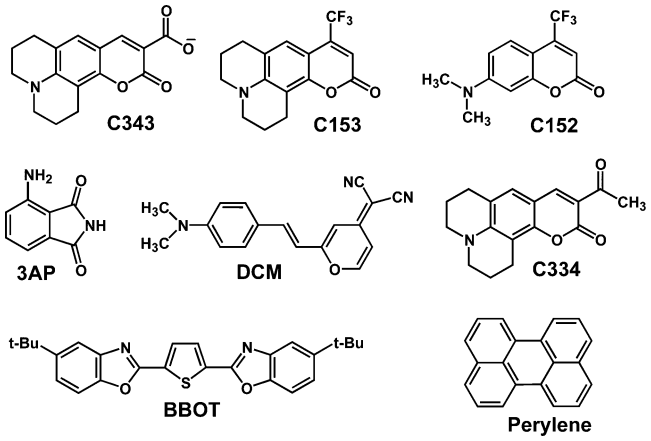

the peak of the lowest absorption band, across the 0.4 mm sample path, was $OD_{max} \leq 0.5$ (only with DCM, the value was $OD_{max} \approx 1$). Optical excitations at 400 nm (~3 μJ) and 267 nm (~0.8 μJ) were second and third harmonics of the main amplified beam at 800 nm (500 Hz). Pulses of 450 and 435 nm (~1 μJ) were generated with a collinear optical parametric amplifier (TOPAS, Light Conversion). Transient fluorescence spectra of the samples were measured with a 1 s integration time. The average of 16 time scans was corrected for photometric and temporal instrument factors, and by multiplication with λ^2, the fluorescence quantum distribution over frequency was obtained as a function of time. Since amplitude information is not needed, measurements were only performed at perpendicular polarization between pump and detection to minimize the solvent Raman signal. An 80 fs (fwhm) time resolution is determined from the intensity cross-correlation between the gate and the pump pulses which have passed through the sample cell and also from the Raman signal.

RESULTS

Polar Solutes. We begin with polar solutes in aprotic polar solvents, namely, acetonitrile and acetone. Excitation wavelengths were limited mainly to 400 and 450 nm. To vary the excess vibrational energy, we therefore work with a number of dyes having different S_1-S_0 energy gaps. In this way the excitation is scanned across the absorption band. Parts a and b of Figure 1 show time-gated fluorescence spectra of C153 and DCM in acetonitrile. With excitation at 400 nm the excess energies of these two probes are estimated (below) at 2780 and 5900 cm^{-1}, respectively. Peak positions are generally determined by log-normal fits. A close look at the spectral evolution reveals that, instead of a monotonous move to the red, the band reaches its maximal red shift at about 2 ps and then reverses toward the blue. For the polar dyes which were examined in acetonitrile, the peak frequencies ν_p as a function of time are compared in Figure 1c. Directly after excitation, they all exhibit a fast decrease which reflects the reorientational dynamics of the solvent, but as a novel finding, once the excitation energy exceeds the 0–0 transition significantly, then the emission band becomes more red-shifted transiently than in its stationary state. The latter is reached by a reverse, blue, shift on a 10 ps time scale.

The bandwidth evolution of C153 in acetonitrile is presented in Figure 2 for excitation at 400 and 450 nm. Shown is the parameter Δ from log-normal fits.[1] As a general observation, excitation with excess vibrational energy causes fast broadening

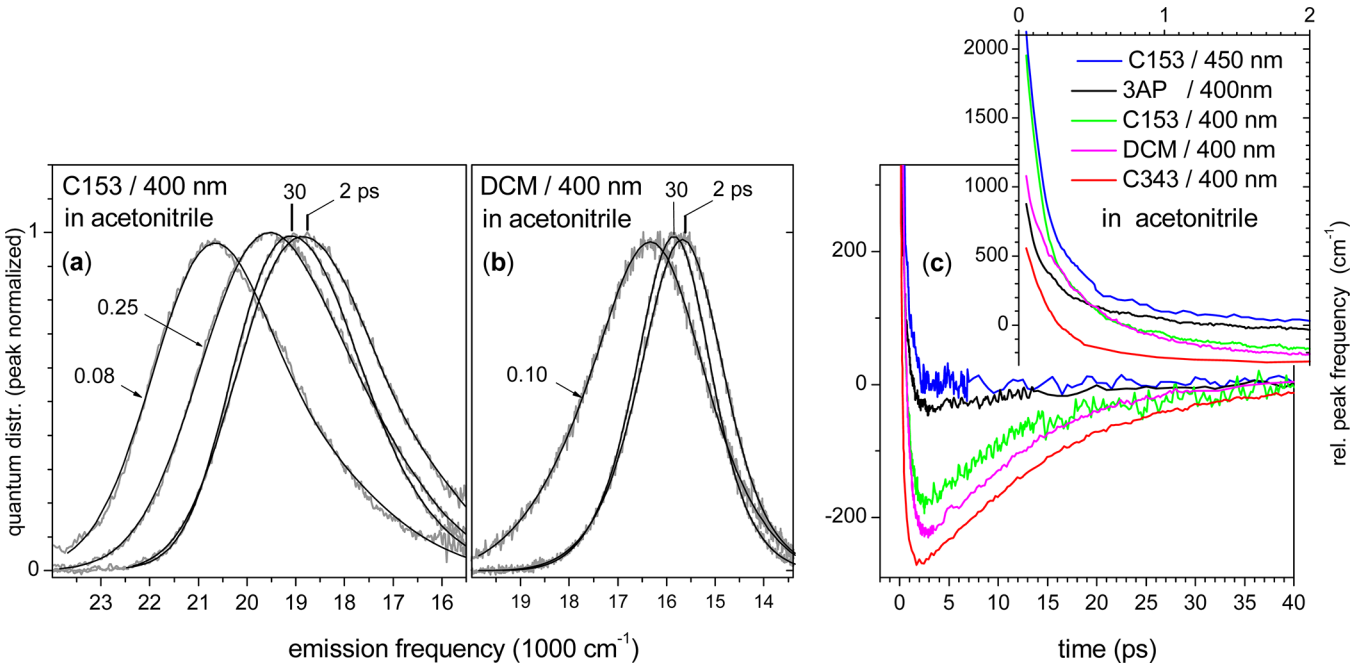

Figure 1. (a) Transient fluorescence spectra of C153 in acetonitrile following 400 nm excitation. Shown are quantum distributions over wavenumbers together with their log-normal fits. For better comparison they are normalized at the peak. At 2 ps the spectrum is more red-shifted than at 30 ps. (b) With DCM under the same conditions, a reverse blue shift is similarly observed from 2 to 30 ps. (c) Peak frequency dynamics of the fluorescence bands of C153, 3AP, C343, and DCM. With optical excitation at 400 nm in common, the excess vibrational energy deposited into the S_1 state differs for these cases. Emission bands undergo an excess red shift, followed by a blue shift to the stationary state. Shown is the peak wavenumber relative to its quasi-stationary value at late time.

dx.doi.org/10.1021/jp400473n | J. Phys. Chem. B 2013, 117, 7675–7684

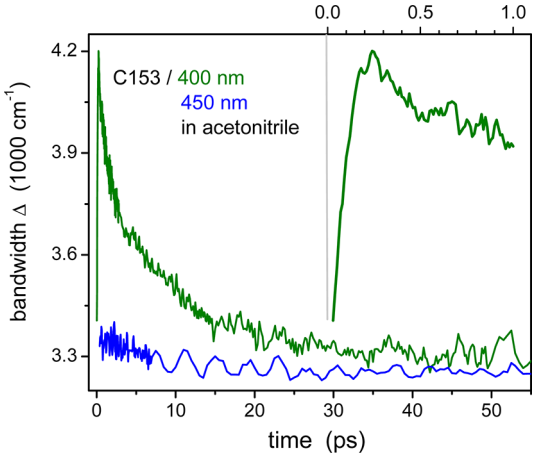

Figure 2. Evolution of the bandwidth parameter Δ of C153 in acetonitrile, following 400 and 450 nm excitations.

of the fluorescence band within $\tau \approx 100$ fs, followed by narrowing on a $\tau \approx 10$ ps time scale. The curves $\nu_p(t)$, $\Delta(t)$, and $\gamma(t)$ (asymmetry parameter) were all fitted by multi-exponential time functions, and the optimal parameters are collected in Tables 1−3.

The effect observed in the peak frequencies appears to be rather general, independent of the polar dye which is used in acetonitrile. It clearly depends on the excess vibrational energy E_{vib} deposited in a molecule (see Figure 3a, which illustrates how our excitation conditions relate to a typical absorption band). Transient fluorescence spectra, as fitted with log-normal functions, are extrapolated reasonably to $t = 0$. In this way the spectrum at time zero is constructed. Then the band shape functions for absorption and emission are calculated and normalized, and the electronic origin transition 00 is taken to correspond to their intersection. The excess S_1 vibrational energy upon optical excitation is also translated into an initial molecular temperature (see the discussion below); a generic model of harmonic modes is used for this purpose.[24] In Figure 3b the excess red shift is plotted against the intramolecular temperature (black symbols, lower x-axis). The excess shift is defined as the peak frequency difference between the fluorescence quantum distribution at the stationary state and the most red-shifted distribution. Coumarins and 3AP fall roughly on a line, whereas DCM appears to behave differently upon excitation at 400 and 450 nm. In acetone the spectral evolution of DCM excited with ~5400 cm^{-1} vibrational energy (not shown) has dynamics similar to that in acetonitrile.

The initial red shift of the peak frequency is described by the terms $\Delta\nu_1 \exp(-t/\tau_1) + \Delta\nu_2 \exp(-t/\tau_2)$ in Table 1. The corresponding relaxation time $\langle\tau_{red}\rangle \approx 0.3$ ps in acetonitrile is fairly independent of the excitation wavelength and, as known from many previous studies,[1,12,13] reflects polar solvation; note however that intramolecular vibrational redistribution may also occurr in this time window. The time constant τ_3 for the subsequent blue shift falls into the 11−15 ps range. We also find that, for the same molecular probe, excitation with excess vibrational energy results in a lower value for the peak frequency at the earliest time compared to excitation at the electronic origin. This is shown in Figure 4 for C343 in

Table 1. Multiexponential Fit Parameters of the Time-Dependent Fluorescence Peak Frequency[a] $\nu_p(t)$ for All Probes in This Study ($T_{solvent}$ = 295 K) (the reverse shift is marked by gray parameter fields)

case	solute	solvent	λ_{exc} (nm)	ν_{00} (cm^{-1})	E_{vib}/hc (cm^{-1})	T_{max} (K)	ν_∞ (cm^{-1})	$\Delta\nu_1$	$\Delta\nu_2$ (cm^{-1})	$\Delta\nu_3$	τ_1	τ_2 (ps)	τ_3	$\langle\tau_{solv}\rangle$[b] (ps)
1			400	22240	2780	427	19035	2430	742	-239	0.11	0.62	10.4	0.22
2	**C153**	acn	450	22240	0	295	19035	2369	523	–	0.13	0.66	–	0.23
3		meoh	400	–	–	–	18402	1727	674	752	0.105	0.984	10.97	2.88
4	**C343**	acn	400	21680	3320	456	20396	1012	178.8	-381	0.19	1.93	12.0	0.45
5			450	21680	540	318	20382	949	112	-41	0.21	1.22	11.1	0.31
6	**C152**	meoh	267	–	–	–	19602	395	382	784	0.17	1.19	14.0	7.38
7			400											
8	**C334**	ch[c]	400	22880	2120	–	21658	571	–	-292	0.08	–	10	10
9	**3AP**	acn	400	24500	500	350	21954	861	438	-51	0.1	0.60	10.2	0.26
10			400	19100	5900	534	15860	690	944	-300	0.13	0.60	10.7	0.40
11	**DCM**	acn	450	19100	3120	436	15873	601	834	-211	0.08	0.53	12.4	0.34
12		act	400	–	–	–	15906	846	759	-300	0.26	1.00	9.1	0.63
13		acn	400	–	–	–	23592	138	–	-103	0.68	–	19.7	–
14	**BBOT**[d]	meoh	400	–	–	–	23383	140	-110	85	1.00	10	19.0	–
15		hex	400	–	–	–	23473	101	–	-78	0.47	–	16.7	–
16	**Perylene**[d]	ch	435	–	–	–	21299	–	–	-60	–	–	15.0	–

[a] $\nu_P(t) = \Delta\nu_1 \exp(-t/\tau_1) + \Delta\nu_2 \exp(-t/\tau_2) + \Delta\nu_3 \exp(-t/\tau_3) + \nu_\infty$; [b] $\langle\tau_{solv}\rangle = (\Delta\nu_1\tau_1 + \Delta\nu_2\tau_2)/(\Delta\nu_1 + \Delta\nu_2)$;
[c] average frequency;
[d] peak frequency of strongest vibronic band. rms deviations between the measured data and the fits are < 10 cm^{-1}. Multi-exponential presentations are solely used to fit the experimental results and have no direct physical meaning. ν_{00}, E_{vib} and T_{max} are the estimated 00 transition frequency, the excess vibrational energy deposited into the molecule by optical excitation, and the maximum temperature of the solute, respectively, for solutions in acetonitrile. acn – acetonitrile, act – acetone, ch – cyclohexane, hex – n-hexane, meoh – methanol.

dx.doi.org/10.1021/jp400473n | J. Phys. Chem. B 2013, 117, 7675−7684

Table 2. Multiexponential Fit Parameters of the Time-Dependent Bandwidth Parameter[a] $\Delta(t)$ ($T_{solvent}$ = 295 K) (values pertaining to the reverse shift are marked by gray fields)

case	solute	solvent[c]	λ_{exc} (nm)	Δ_∞ (cm^{-1})	Δ_1 (cm^{-1})	Δ_2 (cm^{-1})	Δ_3 (cm^{-1})	τ_1 (ps)	τ_2 (ps)	τ_3 (ps)	$\langle\tau_{solv}\rangle$[b] (ps)
1	C153	acn	400	3248	-1969	395	572	0.06	0.84	9.34	5.8
2			450	3248	–	–	107	–	–	8.43	8.43
3		meoh	400	2807	-2252	376	638	0.059	0.66	11.5	7.48
4	C343	acn	400	2198	-724	–	680	0.2	–	12.56	12.56
5			450	2198	-10061	–	103	0.065	–	11.7	11.7
6	C152	meoh	267	3249	-362	–	441	0.05	–	8.04	8.04
7			400	3272	-674	–	584	0.11	–	10.78	10.78
8	C334	ch[c]	400	2113	-59	–	139	0.08	–	9.5	9.5
9	3AP	acn	400	3249	-2148	–	181	0.08	–	11.4	11.4
10	DCM	acn	450	2200	–	1210	256	–	0.29	12.63	2.44
11			400	2200	–	1319	211	–	0.27	3.94	0.77

[a] $\Delta(t) = \Delta_1 \exp(-t/\tau_1) + \Delta_2 \exp(-t/\tau_2) + \Delta_3 \exp(-t/\tau_3) + \Delta_\infty$; [b] $\langle\tau_{solv}\rangle = (\Delta_1\tau_1 + \Delta_2\tau_2)/(\Delta_1 + \Delta_2)$.
[c] in this case $\Delta(t)$ is the fwhm shown in **Fig. 6b**. For solvent abbreviations see legend to **Table 1**.

Table 3. Multiexponential Fit Parameters of the Time-Dependent Asymmetry Parameter[a] $\gamma(t)$ ($T_{solvent}$ = 295 K) (values pertaining to the reverse shift are marked by gray fields)

case	solute	solvent[b]	λ_{exc} (nm)	γ_∞ (cm^{-1})	γ_1 (cm^{-1})	γ_2 (cm^{-1})	γ_3 (cm^{-1})	τ_1 (ps)	τ_2 (ps)	τ_3 (ps)
1	C153	acn	400	-0.31	-0.387	–	–	0.08	–	–
2		acn	450	-0.31		c)			c)	
3		meoh	400	-0.356	-0.21	-0.2	0.3	0.08	5.2	12.44
4	C343	acn	400	-0.59	-0.054	–	0.046	0.86	–	22.5
5			450	-0.59		c)			c)	
6	C152	meoh	267	-0.23	-0.08		0.075	4.5	–	12.5
7			400	-0.23	-0.16	–	0.096	1.7	–	19.08
9	3AP	acn	400	-0.35		c)			c)	
10	DCM	acn	450	0	–	–	0.05	–	–	12.7
11			400	0	-0.097	–	0.04	0.79	–	12.9

[a] $\gamma(t) = \gamma_1 \exp(-t/\tau_1) + \gamma_2 \exp(-t/\tau_2) + \gamma_3 \exp(-t/\tau_3) + \gamma_\infty$.
[b] for abbreviations see legend to **Table 1**. [c] no temporal evolution observed.

acetonitrile, where the peak position could be determined even at a 10 fs delay.

To explore the nature of the excess red shift and to understand whether it has inter- or intramolecular origin, transient fluorescence of C343 in acetonitrile was measured as a function of the solvent temperature. The results are also shown in Figure 3b (red points) where the upper *x* axis gives the solvent temperature. The excess red shift is seen to decrease with the *solvent* temperature, contrary to the behavior with the *molecular* temperature.

A study in a protic polar solvent was performed for reference. To this end the dynamic solvation of C152 in methanol was measured with excitation at 400 and 267 nm, Figure 5. Spectral shifts in methanol are slower on average, extending into the 10 ps range and beyond. On the other hand, the excess red shifts observed so far are most pronounced at 2 ps. If the same process takes place in methanol also, then around 2 ps we expect to find a gap between the curves $\nu_p(t)$ in the figure. The two excitations correspond to ~1400 and ~13 900 cm^{-1} excess vibrational energy. Even with this large difference the two relaxation curves are indistinguishable: no excess red shift is found in methanol. The width behaves differently though (see below).

Also a coumarin in a nonpolar solvent was measured to investigate the excess energy effect in the case where long-range interactions between the solute and solvent are absent. Figure 6a shows transient fluorescence spectra of C334 in cyclohexane at 0.1, 0.35, and 100 ps. Excitation at 400 nm corresponds to $E_{vib} \approx 2120$ cm^{-1}. At 0.35 ps the emission band is seen to have its center at lower energy compared to that at 100 ps. The dynamics of the first moment and the bandwidth (fwhm in this case) are also plotted. Analogous to aprotic polar solvents, the emission band undergoes a fast Stokes shift ($\tau \approx 0.1$ ps) to a position below its stationary state, which is then reached by a 10 ps blue shift.

Nonpolar Solutes. With nonpolar solutes the interaction with the environment is dominated by short-range forces. Absorption and emission spectra of BBOT in *n*-hexane are shown in Figure 7. The prominent vibronic structure allows determination of spectral positions with higher precision than

dx.doi.org/10.1021/jp400473n | J. Phys. Chem. B 2013, 117, 7675−7684

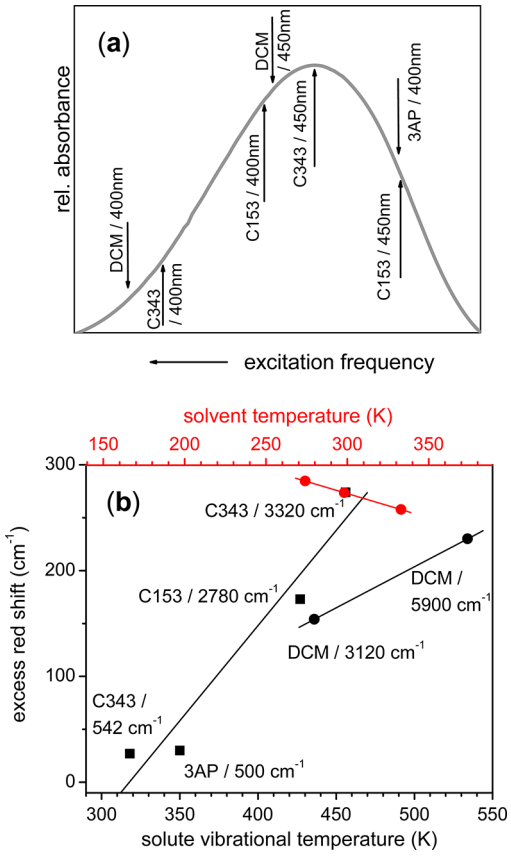

Figure 3. (a) Relative spectral positions for optical excitation of the dyes in acetonitrile on a typical absorption spectrum. (b) Excess red shift depending on the initial S_1 solute temperature (black points, lower abscissa) upon optical excitation in acetonitrile at 298 K. A straight line connects the 3AP, C153, and C343 points. Excess S_1 vibrational energy is indicated. DCM seems to follow a different straight line. Red points refer to DCM when the solvent temperature (upper abscissa) is varied; excitation at 400 nm corresponds to 5900 cm^{-1} excess energy in this case.

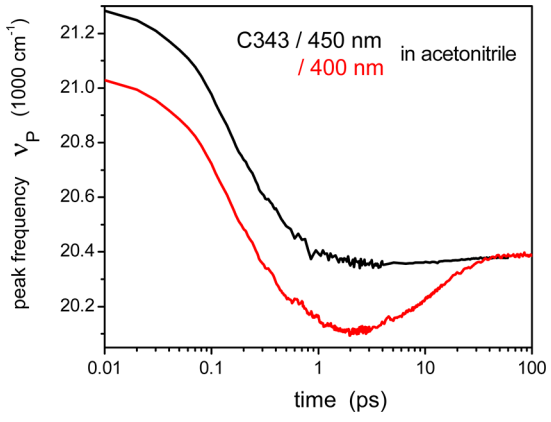

Figure 4. The Stokes shift of C343 in acetonitrile has the same extent for 450 and 400 nm excitation, but the highest and lowest peak positions are different.

for polar probes. In the figure the stationary fluorescence (dashed line) is compared with the upconverted one at 2 ps (solid gray). Differences in the spectral shape for $\nu \leq 23\,500$ cm^{-1} can be attributed to photometric inaccuracy of the upconversion experiment. At higher frequencies a cutoff filter

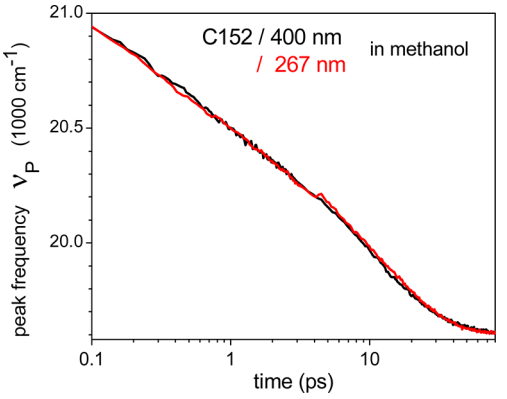

Figure 5. The spectral relaxation of C152 in methanol is identical for excitation at 400 and 267 nm.

has reduced the 00 band for emission, but from the figure one sees directly that the relative peak motion can be followed with about ±5 cm^{-1} precision in this case. BBOT was excited at 400 nm in *n*-hexane, acetonitrile, and methanol, i.e., effectively at the electronic origin in these solvents.[25] The same situation applies to perylene excited at 435 nm in cyclohexane (see the Supporting Information). The peak frequency dynamics $\nu_p(t)$ for the strongest vibronic emission band of BBOT and for the vibronic band of perylene at 21 300 cm^{-1} are shown in Figure 8. To be sure that the Raman signal is avoided, the data are given from 200 fs onward for BBOT and from 520 fs for perylene. With BBOT/*n*-hexane an ultrafast 80 cm^{-1} red shift of the fluorescence band is discerned (inset) followed by a blue shift with $\tau \approx 16$ ps. The spectral relaxation before ~4 ps is modulated by a 250 cm^{-1} oscillation, stronger in *n*-hexane than in polar solvents. With perylene/cyclohexane the time resolution is lower (~320 fs) for technical reasons, and therefore, only the final blue shift is discerned, which has $\tau \approx 15$ ps. BBOT in acetonitrile shows dynamics similar to those in *n*-hexane, but the amplitude of the Stokes shift is slightly larger (see Table 1), and both the red (0.68 p) and subsequent blue shift (19 ps) are slower. Vibrational coherence in BBOT and perylene has vanished by 5 ps, as shown also by extensive transient absorption measurements. At that time the red shift and broadening are almost maximal.

A curious result appears in the peak motion of BBOT in methanol. As in the previous cases the evolution starts with a fast Stokes shift, here with a time constant of 1 ps. Afterward a 10 ps blue shift is observed which, compared to that of solutions in *n*-hexane and acetonitrile, has a smaller amplitude of ~10 cm^{-1}. At times longer than 23 ps the peak moves toward the red again (with $\tau \approx 20$ ps) and therefore relaxes into the stationary state. The two ν_p curves on top of each other in Figure 8c come from measurements 4 months apart, proving the reproducibility.

DISCUSSION

The preceding work was motivated by our studies of polar solvation of biomolecules[26,18,27] and in ionic liquids.[28−30] In this field, a suitable probe is attached, embedded, or dissolved, and the $S_1 \rightarrow S_0$ emission band is followed over several nanoseconds. Needed is the frequency $\nu_{00}(t)$ of the electronic origin transition as it depends on time. With its help a relaxation function for the electronic band gap is constructed

dx.doi.org/10.1021/jp400473n | J. Phys. Chem. B 2013, 117, 7675−7684

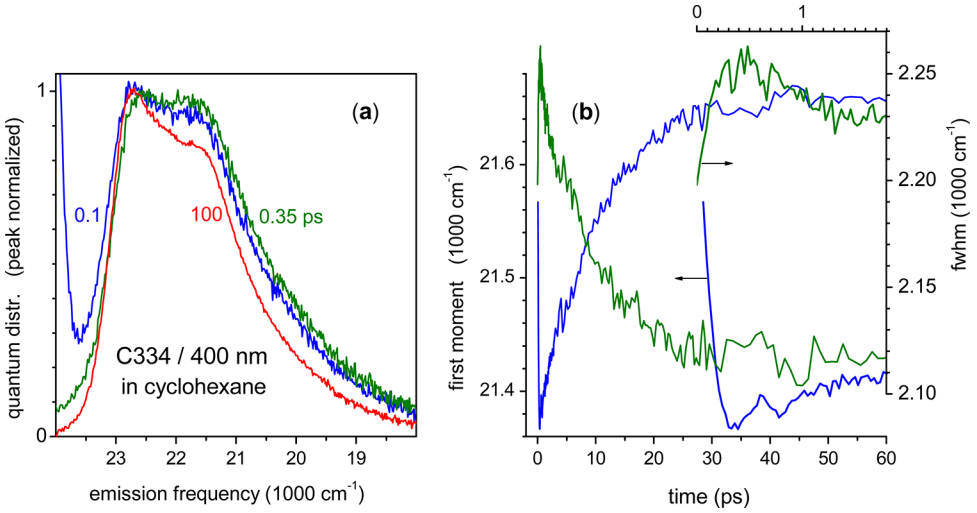

Figure 6. (a) Transient fluorescence spectra of C334 in cyclohexane following 400 nm excitation. Note the effective blue shift at 100 ps compared to 0.1 and 0.35 ps. (b) Dynamics of the first moment (blue lines, left ordinate) and full width at half-maximum (green, right ordinate).

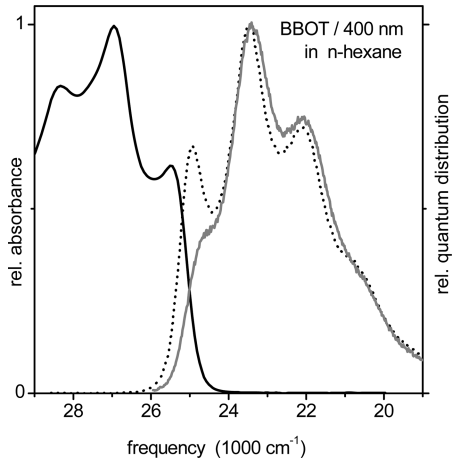

Figure 7. Upconverted fluorescence spectrum of BBOT at 2 ps (gray solid line), compared to the stationary fluorescence (black dashed), in *n*-hexane. Differences for $\tilde{\nu} > 25\,000$ cm^{-1} are due to a cutoff filter which is needed in the time-resolved experiments. The peak position of the dominant vibronic band at a given delay time, relative to the position at some reference time, is determined with ±5 cm^{-1} standard error.

$$S(t) = \frac{\nu_{00}(t) - \nu_{00}(\infty)}{\nu_{00}(0) - \nu_{00}(\infty)} \quad (1)$$

which may be discussed in terms of polar solvent−solute interactions.[13,31−33] In the ideal situation described here, aspects of the liquid motion around the probe are obtained from $S(t)$.[19] Recent results along these lines suggest that the dielectric dispersion $\varepsilon(\omega)$ and conductivity σ_0 can be obtained locally, i.e., in the vicinity of the polarity probe.[30]

However, several obstacles must be overcome before such use of the solvation dynamics is attempted. Most of them relate to the construction of $S(t)$ from the experimental data.

(i) The electronic term value $\nu_{00}(t)$ is not available directly from the observed band envelope. Instead one employs the peak frequency $\nu_p(t)$ or the average frequency $\overline{\nu}(t)$, which may not have the same dynamics.

(ii) At $t = 0$, the Raman signal from the solvent usually swamps the resonance fluorescence from the probe. Therefore, the pertinent $\nu(0)$ which enters into the denominator of eq 1 must be found separately, for example, by comparing stationary absorption and emission spectra with those in a nonpolar solvent.[34]

(iii) The final $\nu(\infty)$ should not be taken simply from the stationary fluorescence spectrum, since the latter is the time average of all transient emission spectra. The parameter must instead be obtained from a fit of the $\nu(t)$ curve. Note that by late times t (typically 10 ns) the population of S_1 has become relatively small and therefore the error in $\nu(\infty)$ can be large, affecting $S(t)$ disproportionately.

(iv) A last problem is the rotational motion of the probe itself.[19] It can be removed through chemical linkage.

By exciting at the blue side of the $S_1 \rightarrow S_0$ absorption band, one expects to overcome obstacle ii since the Raman signal is moved out of the fluorescence window, but as a consequence, excess vibrational energy is deposited into the excited state, and intramolecular vibrational redistribution (IVR) and dissipation to the solvent (cooling) will occur simultaneously with the early stages of solvation. The relaxation function $S(t)$ no longer reflects solvation only. For the most prominent polarity probe, C153, it has been argued[1] that IVR and cooling are reflected primarily by the time-dependent width of the fluorescence band, whereas the peak or average frequencies, $\nu_p(t)$ and $\overline{\nu}(t)$, are unaffected. Studies with C153[1,15,35,36] therefore always employed λ_{exc} = 400 nm, corresponding to ∼2800 cm^{-1} excess vibrational energy. The resulting $S(t)$ curves have been discussed in terms of the structure of the solvation shell and of nonlocal response[37] in light of microscopic theories of solvation. Looking at the variation of $\nu_p(t)$ due to other factors, Figure 1c, we believe that such details are currently beyond the critical reach of experiment.

Excess vibrational energy E_{vib} deposited in the S_1 state appears to be a key variable for the dynamic Stokes shift of fluorescence. Note that, for the most prominent solvation probes, coumarins, the first optical absorption band shows a dense vibronic structure even in the gas phase at low internal temperature, indicating strong vibrational mixing.[38,39] IVR may be considered fast in these cases, on a time scale well below 2 ps. Subsequent cooling takes place with a ∼10 ps time constant, as can be seen for C153/400 nm from the width contraction,

dx.doi.org/10.1021/jp400473n | J. Phys. Chem. B 2013, 117, 7675−7684

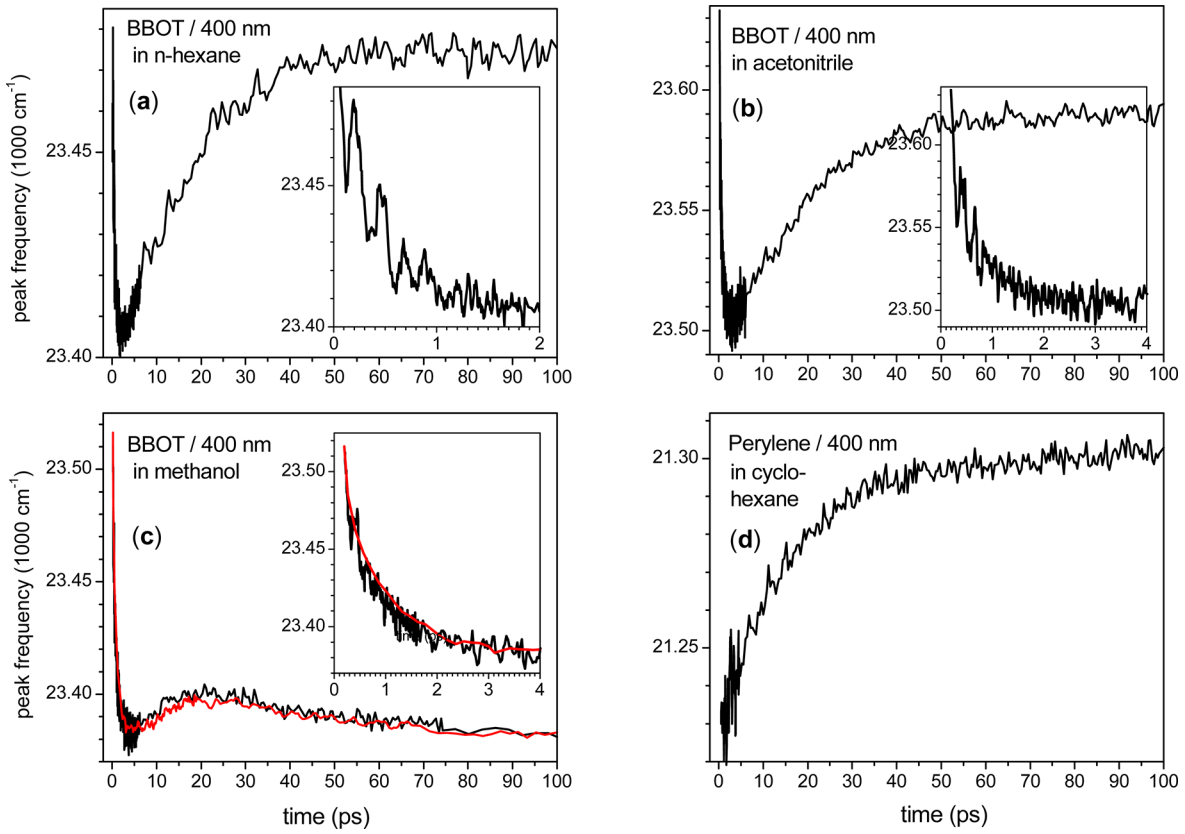

Figure 8. Peak wavenumber of the strongest vibronic band in the fluorescence spectrum of BBOT in (a) *n*-hexane, (b) acetonitrile, and (c) methanol. Transient spectra were evaluated from 200 fs onward to exclude contributions from the excitation pulse. The insets show the initial red-shifting part of the relaxation, seen to be modulated by an intramolecular oscillation with $\tilde{\nu} \approx 250$ cm^{-1}. To check the reproducibility, the measurement in methanol was repeated after 4 months (red line, 200 fs steps only). (d) Peak frequency evolution of the second vibronic band in the transient fluorescence of perylene in cyclohexane. The spectra are evaluated from 500 fs onward.

Figure 2 (green line). The initial increase of the width, with a ~80 fs time constant, probably indicates IVR. That process is not necessarily complete by 200 fs when the width is largest, since some modes may not readily exchange energy with the intramolecular bath of modes.[40] Vibrational coherence in these modes may persist into the picosecond range. However, in C153 the visibility of vibrational coherence in S_1 is quite low after 400 fs,[16] suggesting that only a small fraction of the deposited vibrational energy flows through them. Conversion of E_{vib} into a maximum (initial) temperature T_{max} is therefore allowed.[24] Both E_{vib} and T_{max} have been entered into Table 1 (sixth and seventh columns, respectively).

The excess red shift, $\nu_p(t \approx 2\ \text{ps}) - \nu_p(\infty) < 0$, of the coumarins in acetonitrile is a novel observation, made possible by the steady improvement of broad-band fluorescence techniques.[1,15,17] We see from Figure 3 that the excess shift correlates with the maximal internal temperature of the excited solute. The influence of the excitation wavelength is demonstrated in Figure 4, where $\nu_p(t)$ is shown for C343 in acetonitrile with $\lambda_{exc} = 450$ nm (black) and 400 nm (red curve). The latter curve must contain components due to cooling. In general, we conclude that for solvation studies the optical excitation should be chosen close to the band origin.

The following question remains: Which mechanisms are responsible for the excess red shift when shorter excitation wavelengths are used? Remember that the location of the band origin reflects the state of the environment, independent of the internal molecular temperature. However, the latter affects the band shape, and therefore, the dynamics of $\nu_p(t)$ no longer parallels that of $\nu_{00}(t)$. In the following points (1−3) we briefly discuss scenarios with a view to coumarins.

(1) Transient displacement of tuning modes. With increasing temperature, the high-frequency S_1 vibrational modes which are responsible for the $S_1 \rightarrow S_0$ band envelope (tuning modes) may become more displaced relative to S_0, due to coupling with low-frequency bath modes. This kind of process was originally used in ref 41 to explain fluorescence changes from charge-transfer complexes. As a consequence the FC progression for emission is altered significantly, causing a broader fluorescence envelope with different asymmetry. These changes lead to a red shift of the peak frequency.[42] The effect has been observed with C153 upon static heating;[43] it is here applied to a transient situation. When solvation is fast compared to cooling, the altered emission pattern will sweep to the red as before, but since for solvation at equilibrium the probe is still hot internally, the emission peak at this stage appears more to the red compared to the previous case of 00 excitation. Subsequent cooling restores the original displacement: the envelope regains its former shape, and therefore, the emission peak moves to the blue until the "cold" stationary fluorescence spectrum is reached.

(2) Transient increase of the dipole moment. In the S_1 excited state C153 has several conformations of the substituted amino (julolidine) group, with slightly

dx.doi.org/10.1021/jp400473n | J. Phys. Chem. B 2013, 117, 7675−7684

different dipole moments. Depending on the molecular temperature, the equilibrium between them will be shifted and thus the average dipole moment.[44] Similar conditions are expected for the other push−pull compounds of our study. Referring to the Ooshika−Lippert−Mataga (OLM) equation[45] which connects the dipole moments μ_i in the two electronic states with solvent-induced shifts of ν_{00}, we see that a transient increase $\mu_1 \rightarrow \mu_1 + \Delta\mu_1$ will lead to a transient decrease of ν_{00} and correspondingly of ν_p. This observation applies not only to polar solvents where dipole−dipole interactions dominate, but equally to nonpolar solvents where dipole−induced dipole interactions are responsible for solvent shifts. That polar interactions between the solute and solvent are involved in the excess red shift is also seen from its dependence on the solvent temperature: the red points in Figure 3b show that the shift behaves as $\varepsilon(\omega,T)$ and the simple continuum model prediction.

(3) Transient change of the cavity. For nonpolar solutes only dispersion can stabilize the excited electronic state (multipole interactions typically have the same magnitude and should also be considered here). In a study of stationary absorption and emission of benzene in alkanes, it was concluded that the cavity diameter shrinks by 5−10% upon optical excitation, compared to that in the electronic ground state.[46,47] Coumarin fluorescence spectra are red-shifted by increasing the pressure, as a result of increasing the repulsive forces to the surrounding matrix.[48] We suggest that the time-resolved nonpolar solvations in Figures 6−8 are, at least partly, the transient counterparts of the pressure-induced red shifts. Short-pulse excitation could cause an impulsive excess contraction of the cavity, reflected by the initial red shift. Subsequent relaxation to the excited-state equilibrium then causes the slow blue shift (which in methanol, Figure 8c, is overcompensated by the tail of an overall red shift, probably due to multipole interactions). Note that, with BBOT and perylene in alkanes, no excess energy is involved and vibrational coherence has decayed after a few picoseconds. Even so, the peak shift is well discerned at a later time. Comparing our experimental result with the viscoelastic model of nonpolar solvation developed by Berg,[49] we find similarities for the early fast part of the relaxations with the phonon relaxation dynamics; however, the blue shift with a time constant of ∼15 ps is not predicted by any of the available nonpolar solvation models.[50−53]

Hydrogen bonds with methanol strongly affect the S_0 and S_1 electronic states of all probes discussed so far. Their relative strength is still under discussion even for the best-examined probe, C153 (for a summary the reader is referred to ref 43). Using 4-aminophthalimide, we found that, although half of the reorganization after $S_1 \leftarrow S_0$ excitation (near 00) involves hydrogen bond changes, no signature of that change appears in the dynamic Stokes shift.[54] It was concluded that H-bonds with the solute follow the liquid motion adiabatically. Being coupled both to the intramolecular vibrational motion of the solute and to the collective liquid motion, they are thus a channel for dissipation of excess energy to the environment. Transient temperature-induced changes of the fluorescence band shape or of the excited-state dipole moment might be over completely before 100 fs, providing one possible explanation for the equality of relaxation curves in Figure 5, but the increased width of the emission band (Table 2), which narrows on a picosecond time scale only, suggests otherwise. We are forced to conclude that H-bonding causes the changes in points 1 and/or 2 permanently, regardless of the electronic state and time.

SUMMARY

The solvation dynamics of molecular probes was studied by varying the excess vibational energy upon $S_1 \leftarrow S_0$ optical excitation. In methanol, an excess energy of ∼14 000 cm^{-1} has no effect on the dynamics of the fluorescence Stokes shift.

In aprotic polar solvents such as acetonitrile and acetone, on the other hand, an excess energy as small as 1000 cm^{-1} results in shift dynamics which differs significantly from that of "cold" excitation. The fluorescence band generally shows a transient red shift, exceeding that for the stationary state, followed by a reverse blue shift. The effect is attributed to transient heating of the electronically excited chromophore. This would induce in the excited electronic state (i) an additional displacement of tuning modes or (ii) an additional increase of the dipole moment μ_1.

In the case of nonpolar solutes in nonpolar solvents, even excitation near the electronic origin causes a transient red shift which extends beyond the emission spectrum. This observation could reflect a time dependence of the cavity size of the molecular probe.

The effects of excess vibrational energy in the excited molecular probe, shown here, and also of rotational diffusion examined earlier,[19] should be removed from the dynamic Stokes shift before comparison with liquid theories or MD simulations is made. In general, for solvation studies it is recommended that excitation be done near the band origin.

ASSOCIATED CONTENT

Supporting Information

Absorption spectra of dyes in acetonitrile and methanol. This material is available free of charge via the Internet at http://pubs.acs.org.

AUTHOR INFORMATION

Corresponding Author

*E-mail: sajadi@fhi-berlin.mpg.de (M.S.); nernst@chemie.hu-berlin.de (N.P.E.).

Present Address

†M.S.: Fritz-Haber Institut der Max-Planck-Gesellschaft, Berlin, Germany.

Notes

The authors declare no competing financial interest.

ACKNOWLEDGMENTS

We thank M. Maroncelli for discussions and the Deutsche Forschungsgemeinschaft for financial support (Grant Er 154/9-2).

REFERENCES

(1) Horng, M. L.; Gardecki, J. A.; Papazyan, A.; Maroncelli, M. Subpicosecond Measurements of Polar Solvation Dynamics: Coumarin 153 Revisited. *J. Phys. Chem.* **1995**, *99*, 17311−17337.

(2) Stratt, R. M.; Maroncelli, M. Nonreactive Dynamics in Solution: The Emerging Molecular View of Solvation Dynamics and Vibrational Relaxation. *J. Phys. Chem.* **1996**, *100*, 12981−12996.

(3) Fleming, G. R.; Cho, M. Chromophore-Solvent Dynamics. *Annu. Rev. Phys. Chem.* **1996**, *47*, 109−134.
(4) (a) Ravichandran, S.; Bagchi, B. Orientational Relaxation in Dipolar Systems: How Much Do We Understand the Role of Correlations? *Int. Rev. Phys. Chem.* **1995**, *14*, 271−314. (b) Bagchi, B.; Chandra, A. Collective Orientational Relaxation in Dense Dipolar Liquids. *Adv. Chem. Phys.* **1991**, *80*, 1−126. (c) Bagchi, B. Dynamics of Solvation and Charge Transfer Reactions in Dipolar Liquids. *Annu. Rev. Phys. Chem.* **1989**, *40*, 115−141.
(5) Hsu, C. −P.; Song, X.; Marcus, R. A. Time-Dependent Stokes Shift and Its Calculation from Solvent Dielectric Dispersion Data. *J. Phys. Chem. B* **1997**, *101*, 2546−2551.
(6) Mazurenko, J. T. Electronic-Spectra of 3-Component Solutions. *Opt. Spektrosk.* **1972**, *33*, 1060−1067.
(7) (a) Ware, W. R.; Chow, P.; Lee, S. K. Time-Resolved Nanosecond Emission Spectroscopy: Spectral Shift Due to Solvent-Solute Relaxation. *Chem. Phys. Lett.* **1968**, *2*, 356−358. (b) Ware, W. R.; Lee, S. K.; Brant, G. J.; Chow, P. Nanosecond Time-Resolved Emission Spectroscopy: Spectral Shifts Due to Solvent-Excited Solute Relaxation. *J. Chem. Phys.* **1971**, *54*, 4729−4737.
(8) Barbara, P. F.; Jarzeba, W. Ultrafast Photochemical Intramolecular Charge and Excited State Solvation. *Adv. Photochem.* **1990**, *15*, 1−68.
(9) Jimenez, R.; Fleming, G. R.; Kumar, P. V.; Maroncelli, M. Femtosecond Solvation Dynamics of Water. *Nature* **1994**, *369*, 471−473.
(10) Marroncelli, M. Computer Simulations of Solvation Dynamics in Acetonitrile. *J. Chem. Phys.* **1991**, *94*, 2084−2103.
(11) Ladanyi, B. M.; Stratt, R. M. Short-Time Dynamics of Solvation: Linear Solvation Theory for Polar Solvents. *J. Phys. Chem.* **1995**, *99*, 2502−2511.
(12) Ruthmann, J.; Kovalenko, S. A.; Ouw, D.; Ernsting, N. P. Femtosecond Relaxation of 2-Amino-7-nitrofluorene in Acetonitrile: Observation of the Oscillatory Contribution to the Solvent Response. *J. Chem. Phys.* **1998**, *109*, 5466−5468.
(13) Kumar, P. V.; Maroncelli, M. Polar Solvation Dynamics of Polyatomic Solutes: Simulation Studies in Acetonitrile and Methanol. *J. Chem. Phys.* **1995**, *103*, 3038−3060.
(14) Glasbeek, M.; Zhang, H. Femtosecond Studies of Solvation and Intramolecular Configurational Dynamics of Fluorophores in Liquid Solution. *Chem. Rev.* **2004**, *104*, 1929−1954.
(15) Gustavsson, T.; Cassara, L.; Gulbinas, V.; Gurzadyan, G.; Mialocq, J.-C.; Pommeret, S.; Sorgius, M.; van der Meulen, P. Femtosecond Spectroscopic Study of Relaxation Processes of Three 7-Aminocoumarins in MeOH and DMSO. *J. Phys. Chem. A* **1998**, *102*, 4229−4245.
(16) Eom, I.; Joo, T. J. Polar Solvation Dynamics of Coumarin 153 by Ultrafast Time-Resolved Fluorescence. *Chem. Phys.* **2009**, *131*, 244501−244507.
(17) Zhang, X.-X.; Würth, C.; Zhao, L.; Resch-Genger, U.; Ernsting, N. P.; Sajadi, M. Femtosecond Broadband Fluorescence Upconversion Spectroscopy: Improved Setup and Photometric Correction. *Rev. Sci. Instrum.* **2011**, *82*, 063108−063115.
(18) Sajadi, M.; Ajaj, Y.; Ioffe, I.; Weingärtner, H.; Ernsting, N. P. THz Absorption Spectroscopy of a Liquid via a Polarity Probe. A Case Study of Trehalose/Water Mixtures. *Angew. Chem., Int. Ed.* **2010**, *49*, 454−457.
(19) Sajadi, M.; Weinberger, M.; Wagenknecht, H.-A.; Ernsting, N. P. Polar Solvation Dynamics in Water and Methanol: Search for Molecularity. *Phys. Chem. Chem. Phys.* **2011**, *13*, 17768−17774.
(20) Fourkas, J. T.; Benigno, A.; Berg, M. Time-Resolved Nonpolar Solvation Dynamics in Supercooled and Low-Viscosity n-Butylbenzene. *J. Chem. Phys.* **1993**, *99*, 8552−8558.
(21) Berg, M. Comparison of a Viscoelastic Theory of Solvation Dynamics to Time-Resolved Experiments in a Nonpolar Solution. *Chem. Phys. Lett.* **1994**, *228*, 317−322.
(22) Yu, J.; Berg, M. Solvent-Electronic State Interactions Measured from the Glassy to the Liquid State. I. Ultrafast Transient and Permanent Hole Burning in Glycerol. *J. Chem. Phys.* **1992**, *96*, 8741−8749.
(23) Ma, J.; Vanden Bout, D.; Berg, M. Transient Hole Burning of s-Tetrazine in Propylene Carbonate: A Comparison of Mechanical and Dielectric Theories of Solvation. *J. Chem. Phys.* **1995**, *103*, 9146−9160.
(24) Vibrational modes are assumed to be equally distributed from 0 to 1600 cm^{-1}, except for the C−H stretching modes that have an energy of ∼3000 cm^{-1}; for details see: (a) Nakabayashi, T.; Okamoto, H.; Tasumi, M. Probe-Wavelength Dependence of Picosecond Time-Resolved Anti-Stokes Raman Spectrum of Canthaxanthin: Determination of Energy States of Vibrationally Excited Molecules Generated via Internal Conversion from the Lowest Excited Singlet State. *J. Phys. Chem. A* **1997**, *101*, 3494−3500. (b) See ref 29.
(25) Here we limit the nonpolar solvation study to excitation with ∼0 excess vibrational energy. In a future paper the excitation energy dependence will be examined.
(26) Dallmann, A.; Pfaffe, M.; Mügge, C.; Mahrwald, R.; Kovalenko, S. A.; Ernsting, N. P. Local THz Time-Domain Spectroscopy of Duplex DNA via Fluorescence of an Embedded Probe. *J. Phys. Chem. B* **2009**, *113*, 15619−15628.
(27) Sajadi, M.; Furse, K. E.; Zhang, X.-X.; Dehmel, L.; Kovalenko, S. A.; Corcelli, S. A.; Ernsting, N. P. Detection of DNA-Ligand Binding Oscillations by Stokes-Shift Measurements. *Angew. Chem., Int. Ed.* **2011**, *123*, 6973−9677.
(28) Maroncelli, M.; Zhang, X. −X.; Liang, M.; Roy, D.; Ernsting, N. P. Measurements of the Complete Solvation Response of Coumarin 153 in Ionic Liquids and the Accuracy of Simple Dielectric Continuum Predictions. *Faraday Discuss.* **2012**, *154*, 409−424.
(29) Zhang, X.-X.; Liang, M.; Ernsting, N. P.; Maroncelli, M. Complete Solvation Response of Coumarin 153 in Ionic Liquids. *J. Phys. Chem. B* **2013**, *7*, 1205−1210.
(30) Zhang, X. -X.; Schroeder, C.; Ernsting, N. P. Solvation and Dielectric Response in Ionic Liquids—Conductivity Extension of the Continuum Model. *J. Chem. Phys.* **2013**, *138*, 111102−111103.
(31) Maroncelli, M.; Macinnis, J.; Fleming, G. R. Polar Solvent Dynamics and Electron-Transfer Reactions. *Science* **1989**, *243*, 1674−1681.
(32) Maroncelli, M. The Dynamics of Solvation in Polar Liquids. *J. Mol. Liq.* **1993**, *57*, 1−37.
(33) Bagchi, B.; Oxtoby, D. W.; Fleming, G. R. Theory of the Time Development of the Stokes Shift in Polar Media. *Chem. Phys.* **1984**, *86*, 257−267.
(34) Fee, R. S.; Maroncelli, M. Estimating the Time-Zero Spectrum in Time-Resolved Emission Measurements of Solvation Dynamics. *Chem. Phys.* **1994**, *183*, 235−247.
(35) Changenet-Barret, B.; Choma, C.; Gooding, E.; DeGrado, W.; Hochstrasser, R. Ultrafast Dielectric Response of Proteins from Dynamics Stokes Shifting of Coumarin in Calmodulin. *J. Phys. Chem. B* **2000**, *104*, 9322−9329.
(36) Perez-Lustres, J. L.; Rodriguez-Prieto, F.; Mosquera, M.; Senyushkina, T. A.; Ernsting, N. P.; Kovalenko, S. A. Ultrafast Proton Transfer to Solvent: Molecularity and Intermediates from Solvation- and Diffusion-Controlled Regimes. *J. Am. Chem. Soc.* **2007**, *129*, 5408−5418.
(37) Kashyap, H. K.; Biswas, R. Solvation Dynamics of Dipolar Probes in Dipolar Room Temperature Ionic Liquids: Separation of Ion Dipole and Dipole Dipole Interaction Contributions. *J. Phys. Chem. B* **2010**, *114*, 254−268.
(38) Mühlpfordt, A.; Schanz, R.; Ernsting, N. P.; Farztdinov, V.; Grimme, S. Coumarin 153 in the Gas Phase: Optical Spectra and Quantum Chemical Calculations. *Phys. Chem. Chem. Phys.* **1999**, *1*, 3209−3218.
(39) (a) Pryor, B. A.; Andrews, P. M.; Palmer, M. P.; Berger, M. R.; Topp, M. R. Spectroscopy of Jet-Cooled Water Complexes with Coumarin 151: Observation of Vibronically Induced Conformational Barrier Crossing. *J. Phys. Chem.* **1998**, *102*, 3284−3292. (b) Pryor, B. A.; Palmer, P. M.; Chen, Y.; Topp, M. R. Identification of Dual Conformers of Coumarin 153 under Jet-Cooled Conditions. *Chem. Phys. Lett.* **1999**, *299*, 536−544.

(40) Weston, R. E.; Barker, J. R. On Modeling the Pressure-Dependent Photoisomerization of *trans*-Stilbene by Including Slow Intramolecular Vibrational Energy Redistribution. *J. Phys. Chem. A* **2006**, *110*, 7888−7897.
(41) Rubtsov, I. V.; Yoshihara, K. Vibrational Coherence in Electron Donor-Acceptor Complexes. *J. Phys. Chem. A* **1999**, *103*, 10202−10212.
(42) Mertz, E. L. On the Dependence of the Electron Band Maximum on the Solvent Reorganization Energy. *Chem. Phys. Lett.* **1996**, *262*, 27−32.
(43) (a) Tomczak, J.; Dobek, K. Coumarin 153 Emission Thermochromism Studied in Non-Specifically and Specifically Interacting Solvents. *J. Lumin.* **2009**, *129*, 884−891. (b) Dobek, K. The Influence of Temperature on Coumarin 153 Fluorescence Kinetics. *J. Fluoresc.* **2011**, *21*, 1547−1557. (c) Dobek, K.; Karolczak, J. The Influence of Temperature on C153 Steady-State Absorption and Fluorescence Kinetics in Hydrogen Bonding Solvents. *J. Fluoresc.* **2012**, *22*, 1647−1657.
(44) Ingrosso, F.; Ladanyi, B. M.; Mennucci, B.; Elola, M. D.; Tomasi, J. Solvation Dynamics in Acetonitrile: A Study Incorporating Solute Electronic Response and Nuclear Relaxation. *J. Phys. Chem. B* **2005**, *109*, 3553−3564.
(45) Mataga, N., Kubota, T. *Molecular Interactions and Electronic Spectra*; Marcel Dekker, Inc.: New York, 1970.
(46) Li, F.; Lee, J.; Bernstein, E. R. Absorption and Emission Spectroscopy of Benzene in Cryogenic Solutions: An Estimate of the Intermolecular Potential. *J. Phys. Chem.* **1982**, *86*, 3606−3611.
(47) Nowak, R.; Bernstein, E. R. Spectroscopic Studies of Cryogenic Fluids: Benzene in Propane. *J. Chem. Phys.* **1987**, *86*, 3197−3206.
(48) Kutty, A. P. G.; Venkateswaran, S.; Vaidya, S. N.; Kartha, V. B. Pressure Effects on Absorption and Fluorescence of Polar Dyes. *J. Phys. Chem.* **1993**, *97*, 7132−7134.
(49) Berg, M. Viscoelastic Continuum Model of Nonpolar Solvation. 1. Implications for Multiple Time Scales in Liquid Dynamics. *J. Phys. Chem. A* **1998**, *102*, 17−30.
(50) Larsen, R. E.; David, E. F.; Goodyear, G.; Stratt, R. M. Instantaneous Perspectives on Solute Relaxation in Fluids: The Common Origins of Nonpolar Solvation Dynamics and Vibrational Population Relaxation. *J. Chem. Phys.* **1997**, *107*, 524−543.
(51) Matyushov, D. V.; Schmid, R. Optical and Radiationless Intramolecular Electron Transitions in Nonpolar Fluids: Relative Effects of Induction and Dispersion Interactions. *J. Chem. Phys.* **1995**, *103*, 2034−2049.
(52) Walsh, A. M.; Loring, R. F. Photon Echoes in a Nonpolar Fluid. *Chem. Phys. Lett.* **1991**, *186*, 77−83.
(53) Bagchi, B. Molecular Theory of Nonpolar Solvation Dynamics. *J. Chem. Phys.* **1994**, *100*, 6658−6664.
(54) Sajadi, M.; Obernhuber, T.; Kovalenko, S. A.; Mosquera, M.; Dick, B.; Ernsting, N. P. Dynamic Polar Solvation Is Reported by Fluorescing 4-Aminophthalimide Faithfully Despite H-Bonding. *J. Phys. Chem. A* **2009**, *113*, 44−55.